

Study of the nonelementary singular points and the dynamics near the infinity in predator-prey systems

Érika Diz-Pita, Jaume Llibre and M. Victoria Otero-Espinar

Abstract In this chapter we present the results obtained in two predator-prey systems, paying special attention to the dynamics near the infinity and the nonelementary singular points. First, the desingularization technique known as blow up technique, allows one to study any type of singularities of analytic systems in dimension two even if they are not elementary. In the other hand, the introduction of the Poincaré compactification allows one to accomplish a complete study of the global dynamics of these systems. In addition to the proofs of the results obtained in those cases, we include a survey on the used techniques from a theoretical point of view.

1 Introduction

Dynamical systems that represent the interaction between coexisting species, as it is the particular case of predator-prey systems, have been widely studied in the literature. Starting from the most classical models, such as the one proposed by A. Lotka [1] and V. Volterra [2], researchers have made efforts to add new features to these models, making them more realistic and allowing them to be adapted to more real-world situations.

In [3] different proposals for modeling predator-prey systems have been studied comparatively. Special attention has been paid to the inclusion of characteristics such as the Allee effect, immigration, fear and, in general, to the indirect effects that the presence of predators can produce on prey, apart from direct attack.

Érika Diz-Pita
Universidad Intercontinental de la Empresa, e-mail: erika.diz@uie.edu

Jaume Llibre
Universitat Autònoma de Barcelona e-mail: jllibre@mat.uab.cat

M.Victoria Otero-Espinar
Universidad de Santiago de Compostela e-mail: mvictoria.otero@usc.es

One thing that can be appreciated is that, while trying to make the models more realistic from a biological and ecological point of view, from a mathematical point of view appear more difficulties in the study of these differential systems.

For example, there are many population models focused on the analysis of finite singular points and their stability, but especially in hyperbolic cases. We will give a summary on a desingularization technique that can improve or complete the existing works in the sense that it allows one to study any type of singularities even if they are not elementary.

On the other hand, we will also present the Poincaré compactification which allows one to accomplish a complete study of the global dynamics of the systems, making possible to know the behavior of the orbits in a neighborhood the infinity.

In addition to the description of these techniques from a theoretical point of view, we present two systems in the field of population dynamics to which we have applied them, and we present the results obtained.

The first model we have studied is obtained from the classical Rosenzweig and MacArthur model, introduced in [4]. Considering $x \geq 0$ as the prey density and $y \geq 0$ as the predator density, the original model has the form

$$\begin{aligned}\dot{x} &= rx \left(1 - \frac{x}{K}\right) - y \frac{mx}{b+x}, \\ \dot{y} &= y \left(-\delta + c \frac{mx}{b+x}\right),\end{aligned}$$

where the parameter $\delta > 0$ represents the death rate of the predator species and $c > 0$ is the rate of conversion of prey to predator. In this system, the functional response is given by the function $mx/(b+x)$, so it is a Holling type II functional response.

As we can see with detail in [5], the previous system can be reduced to a polynomial differential system. Summarizing it is necessary to do a rescaling $(\bar{x}, \bar{y}, \bar{b}, \bar{c}, \bar{\delta}) = (x/K, (m/rK)y, b/K, cm/r, \delta/r)$ and a time rescaling multiplying by $b+x$. Thus a polynomial system of degree three is obtained, being b , c and δ positive parameters:

$$\begin{aligned}\dot{x} &= x(-x^2 + (1-b)x - y + b), \\ \dot{y} &= y((c-\delta)x - \delta b).\end{aligned}\tag{1}$$

This is a particular case of Kolmogorov systems, which were proposed in [6] as an extension of the Lotka-Volterra systems to arbitrary dimension and degree. Kolmogorov systems are differential systems of the form

$$\dot{x}_i = x_i P_i(x_1, \dots, x_n), \quad i = 1, \dots, n,$$

where P_i are polynomials. The techniques we are describing in this chapter have been used to classify all the global dynamics of some families of general Kolmogorov systems in [7, 8, 9, 10].

We study system (1) in the positive quadrant of the plane \mathbb{R}^2 where it has ecological meaning, more precisely, we wanted to complete the study of the dynamics of system

(1) and classify all their phase portraits on the closed positive quadrant of the Poincaré disc, that we will introduce later on, so in this way we can control the dynamics of the system near the infinity. More details can be found in [11].

The second system we will consider in this chapter is the system

$$\begin{aligned}\dot{x} &= x \left(a_0 + c_1 x + c_2 z^2 + c_3 z \right), \\ \dot{z} &= z \left(c_0 + c_1 x + c_2 z^2 + c_3 z \right),\end{aligned}\tag{2}$$

This system, which is also a Kolmogorov system, is important as it has been obtained from a general Lotka-Volterra system on dimension three. Those kind of Lotka-Volterra systems have been used for modelling different problems as in hydrodynamics [12], chemical reactions [13], economic and social problems [14, 15, 16]. They have been also used in the field in which we are focusing our attention: population dynamics. For example, the interaction between species has been modeled with these kind of systems in [17, 18, 19, 20, 21].

Only very particular cases of Lotka-Volterra systems in dimension three had been studied, as for example the cases in [22], where the authors give the global phase portraits in the Poincaré ball of a system related with the study of black holes or in [23], where the authors study a family depending only on two parameters.

In view of the lack of general results, and although the complete study of all these systems does not seem directly approachable, it seemed interesting to address the study of larger classes of systems within the Lotka-Volterra in dimension three. From general 3-dimensional Lotka-Volterra systems depending on 12 parameters, we have obtained two big subfamilies in [7] by applying the Darboux theory of integrability.

System (2) corresponds with one of those subfamilies by setting the value of one of the parameters equal to -1 . We present this particular case as it has a line of singular points at infinity, i.e., all the infinity is filled up with singular points. We consider this system interesting as there are few works that study these kind of systems when they have a line filled up of singular points.

Next, in Section 3, we describe the desingularization technique using directional blow ups, and then apply it to the systems that we have just presented. With the same structure, we describe the Poincaré compactification in Section 2, and apply it to both systems, explaining the results obtained.

2 The dynamics near the infinity

Many systems used in population dynamics are planar systems, for example, all those which deal with the evolution of a predator species and a prey species that coexist. When trying to study the behavior of those systems in the whole plane \mathbb{R}^2 , an obvious difficulty arises if we try to define what happens globally, because we cannot fully control the orbits as they go to or come from infinity.

What we present here is a special kind of compactification, which can be used provided that the functions defining the vector field are polynomials. This technique, introduced by Poincaré [24], allows one to control the orbits which tend to or come from infinity, and to draw the phase portrait in a finite region, the sphere \mathbb{S}^2 , or even simpler, in the planar disk \mathbb{D}^2 .

In the following we describe the construction of this compactification for a general polynomial system, and then we apply it to the predator-prey systems given in Section 1.

2.1 The Poincaré compactification

Let consider a polynomial vector field of degree d of the form:

$$X = P \frac{\partial}{\partial x_1} + Q \frac{\partial}{\partial x_2},$$

where P and Q are polynomials such that d is the maximum of the degrees of P and Q . Let consider that the variables of the polynomial are x_1 and x_2 , so the vector field defines a polynomial differential system of the form

$$\begin{aligned} \dot{x}_1 &= P(x_1, x_2), \\ \dot{x}_2 &= Q(x_1, x_2). \end{aligned} \tag{3}$$

For this polynomial system we give the construction of the Poincaré compactification. The main idea is that we want to project our vector field from an infinite surface, which is \mathbb{R}^2 onto the bounded surface of the sphere $\mathbb{S}^2 = \{y \in \mathbb{R}^3 : y_1^2 + y_2^2 + y_3^2 = 1\}$. Thus, we can place \mathbb{R}^2 as a tangent plane to the sphere at the point $(0, 0, 1)$, i.e., we consider \mathbb{R}^2 as the plane in \mathbb{R}^3 defined by $(y_1, y_2, y_3) = (x_1, x_2, 1)$. We call the *Poincaré sphere* to the sphere \mathbb{S}^2 , which is usually divided into three regions: the northern hemisphere,

$$H_+ = \{y \in \mathbb{S}^2 : y_3 > 0\};$$

the southern hemisphere,

$$H_- = \{y \in \mathbb{S}^2 : y_3 < 0\};$$

and the equator

$$\mathbb{S}^1 = \{y \in \mathbb{S}^2 : y_3 = 0\}.$$

Now we need a way to project what is on \mathbb{R}^2 onto the Poincaré sphere. For doing that we can consider the central projections $f^+ : \mathbb{R}^2 \rightarrow \mathbb{S}^2$ and $f^- : \mathbb{R}^2 \rightarrow \mathbb{S}^2$.

The image $f^+(x)$ of a point x is defined as the intersection of the straight line passing through the point x and the origin with the northern hemisphere of \mathbb{S}^2 , and respectively, the image $f^-(x)$ of a point x is the intersection of the straight

line passing through the point x and the origin with the southern hemisphere. The analytical expressions of these projections are

$$f^+(x) = \left(\frac{x_1}{\Delta(x)}, \frac{x_2}{\Delta(x)}, \frac{1}{\Delta(x)} \right), \quad f^-(x) = \left(\frac{-x_1}{\Delta(x)}, \frac{-x_2}{\Delta(x)}, \frac{-1}{\Delta(x)} \right),$$

where $\Delta(x) = \sqrt{x_1^2 + x_2^2 + 1}$.

With the differential of these projections we obtain induced vector fields in the northern and southern hemispheres. The induced vector field on H_+ is

$$\bar{X}(y) = Df^+(x)X(x), \quad \text{where } y = f^+(x),$$

and the one in H_- is

$$\bar{X}(y) = Df^-(x)X(x), \quad \text{where } y = f^-(x).$$

Now we have a vector field on $\mathbb{S}^2 \setminus \mathbb{S}^1$, that we name by \bar{X} , that is everywhere tangent to \mathbb{S}^2 .

But our motivation for doing this compactification was to study the dynamics of the orbits in a neighborhood of the infinity. Note that the points at the infinity of \mathbb{R}^2 are in bijective correspondence with the points of the equator of \mathbb{S}^2 , and for the moment our induced vector field \bar{X} is not defined over the equator.

So the next step is to carry out this extension of the induced vector field \bar{X} from $\mathbb{S}^2 \setminus \mathbb{S}^1$ to \mathbb{S}^2 . In general, the field is not bounded as we get close to \mathbb{S}^1 so, to make possible the extension, we should multiply the vector field by the factor $\rho(x) = x_3^{d-1}$ and then the extension is feasible.

In short, we call the *Poincaré compactification* of the vector field X on \mathbb{R}^2 to this extended vector field, and we denote it by $\rho(X)$.

Once the idea of this method has been exposed, we need to specify what will be the expression of this compactification, in order to be able to work with it, as we will do later on with the predator-prey systems. As we are working on a surface \mathbb{S}^2 , to make calculations we need to use local charts in the surface.

We consider the six local charts of \mathbb{S}^2 given by

$$U_i = \{y \in \mathbb{S}^2 \mid y_k > 0\}, \quad V_i = \{y \in \mathbb{S}^2 \mid y_k < 0\},$$

and the local maps

$$\phi_k : U_k \longrightarrow \mathbb{R}^2 \quad \text{and} \quad \psi_k : V_k \longrightarrow \mathbb{R}^2,$$

for $i = 1, 2, 3$. The previous maps are defined by

$$\phi_i(y) = \psi_i(y) = \left(\frac{y_m}{y_i}, \frac{y_n}{y_i} \right),$$

with $m < n$ and $m, n \neq i$. We denote by $z = (u, v)$ the value of the maps $\phi_i(y)$ or $\psi_i(y)$, for any value of i . Then (u, v) has different roles depending on the selected local chart. Geometrically the coordinates (u, v) can be expressed as in Figure 1. In all the charts, the points which are over the equator have the coordinate $v = 0$.

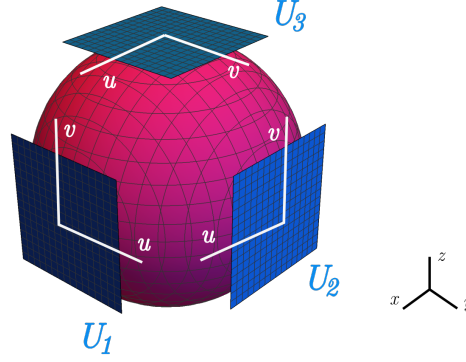


Fig. 1: : The Poincaré sphere with the local charts (U_j, ϕ_j) for $j = 1, 2, 3$.

Let consider the chart U_1 and let calculate the expression of $\rho(X)$ in this chart (see [25]). Our initial polynomial vector field was

$$X(x) = (P(x_1, x_2), Q(x_1, x_2))$$

and with the central projection f^+ we get the vector field on the northern hemisphere

$$\bar{X}(y) = Df^+(x)X(x) \text{ with } y = f^+(x),$$

with the local map ϕ_1 :

$$D\phi_1(y)\bar{X}(y) = D\phi_1(y) \circ Df^+(x)X(x) = D(\phi_1 \circ f^+)(x)X(x).$$

Then

$$(\phi_1 \circ f^+)(x) = \phi_1 \left(\frac{x_1}{\Delta(x)}, \frac{x_2}{\Delta(x)}, \frac{1}{\Delta(x)} \right) = \left(\frac{x_2}{x_1}, \frac{1}{x_1} \right) = (u, v),$$

and

$$D(\phi_1 \circ f^+)(x) = \begin{pmatrix} -\frac{x_2}{x_1^2} & \frac{1}{x_1} \\ -\frac{1}{x_1^2} & 0 \end{pmatrix}.$$

If we denote by $\bar{X}|_{U_1}$ the system defined as $D\phi_1(y)\bar{X}(y)$, we have

$$\bar{X}|_{U_1} = \begin{pmatrix} -\frac{x_2}{x_1^2} & \frac{1}{x_1} \\ -\frac{1}{x_1^2} & 0 \end{pmatrix} \begin{pmatrix} P(x_1, x_2) \\ Q(x_1, x_2) \end{pmatrix},$$

and so the components of the field can be expressed as

$$\begin{aligned} \bar{X}|_{U_1} &= \begin{pmatrix} -\frac{x_2}{x_1^2} P(x_1, x_2) + \frac{1}{x_1} Q(x_1, x_2), -\frac{1}{x_1^2} P(x_1, x_2) \end{pmatrix} \\ &= \frac{1}{x_1^2} (-x_2 P(x_1, x_2) + x_1 Q(x_1, x_2), -P(x_1, x_2)). \end{aligned}$$

Also

$$\rho(y) = y_3^{d-1} = \left(\frac{1}{\Delta(x)} \right)^{d-1} = \left(\frac{1}{x_1} \right)^{d-1} m(z),$$

where

$$m(z) = \left(1 + \left(\frac{x_2}{x_1} \right)^2 + \left(\frac{1}{x_1} \right)^2 \right)^{\frac{1-d}{2}}.$$

We can multiply the field $\bar{X}|_{U_1}$ by $\rho(y)$, which is equivalent to change the time variable t for a new variable s , so that $dt = \rho(y)ds$, and the only change on the phase portrait is the velocity at which orbits are traveled.

Now we have a compactification of the field on the local charts that has a well defined polynomial expression

$$\rho(y)(\bar{X}|_{U_1}) = \frac{m(z)}{x_1^2} (-x_2 P(x_1, x_2) + x_1 Q(x_1, x_2), -P(x_1, x_2)),$$

and, although $\bar{X}|_{U_1}$ is not defined when at the points of the equator, $p(X)|_{U_1} = \rho\bar{X}|_{U_1}$ is well defined at the infinity, so the extension of $\rho\bar{X}$ to $p(X)$ is defined on the whole of \mathbb{S}^1 . Moreover, in order to simplify the extended vector field we also make a change in the time variable and remove the factor $m(z)$.

If the variables in the local charts are (u, v) , the Poincaré compactification of the vector field X is given by

$$\begin{aligned} \dot{u} &= v^d \left[-u P\left(\frac{1}{v}, \frac{u}{v}\right) + Q\left(\frac{1}{v}, \frac{u}{v}\right) \right], \\ \dot{v} &= -v^{d+1} P\left(\frac{1}{v}, \frac{u}{v}\right), \end{aligned} \tag{4}$$

in local chart (U_1, ϕ_1) . In (U_2, ϕ_2) we have

$$\begin{aligned}\dot{u} &= v^d \left[P\left(\frac{u}{v}, \frac{1}{v}\right) - uQ\left(\frac{u}{v}, \frac{1}{v}\right) \right], \\ \dot{v} &= -v^{d+1} Q\left(\frac{u}{v}, \frac{1}{v}\right),\end{aligned}\tag{5}$$

and finally, in (U_3, ϕ_3) :

$$\begin{aligned}\dot{u} &= P(u, v), \\ \dot{v} &= Q(u, v).\end{aligned}\tag{6}$$

Even the complete geometrical construction is important to understand the idea of this method, once we want to apply it to some particular equations we can obtain the expression in the following way.

To obtain (4) we start with (3) and introduce coordinates (u, v) by the formulas $(x_1, x_2) = (1/v, u/v)$. This leads to a vector field \bar{X}^u which we must multiply by v^{d-1} .

To obtain (5) we start with (3) and introduce coordinates (u, v) by the formulas $(x_1, x_2) = (u/v, 1/v)$. We again multiply the obtained vector field \bar{X}^v by v^{d-1} .

The expressions in (6) do not need any elaboration, and we just have to replace (x_1, x_2) by (u, v) .

In the remaining charts (V_k, ψ_k) , with $k = 1, 2, 3$, the expression for $\rho(X)$ is the same as for (U_k, ϕ_k) but multiplied by $(-1)^{d-1}$. Therefore, it is not necessary to study the system in these charts, as it is enough to determine the behavior of the orbits based on the behavior on the charts (U_i, ϕ_i) , with $i = 1, 2, 3$.

We recall that the importance of this compactification relies on the fact that the points at the infinity of \mathbb{R}^2 are now the finite point on the equator of the sphere. All the singular points of $\rho(X)$ which lie in the equator are called the *infinite singular points* of X , and the following result holds:

Proposition 1 *If $y \in \mathbb{S}^1$ is an infinite singularity of the Poincaré compactification $\rho(X)$ of a field X , then the opposite point $-y$ is an infinite singularity of the compactification $\rho(X)$ and both singularities have the same stability if the degree of vector field is odd; they have opposite stability if the degree is even.*

As mentioned in the introduction we can make a new projection that simplifies the representation of the phase portraits. The idea is now to project the northern hemisphere of \mathbb{S}^2 onto the plane $y_3 = 0$ with the orthogonal projection π . The image of the hemisphere is called the *Poincaré disk*, and we denote it by \mathbb{D}^2 .

It will be enough to study the system in the Poincaré disk since the orbits of $\rho(X)$ on \mathbb{S}^2 are symmetric with respect to the origin of \mathbb{R}^3 , so we only need to consider the flow of $\rho(X)$ in the closed northern hemisphere. In Figure 2 we include the Poincaré disk with the charts U_1, U_2, v_1 and V_2 , and in the examples that we will provide, we will also include the phase portraits in the Poincaré disk.

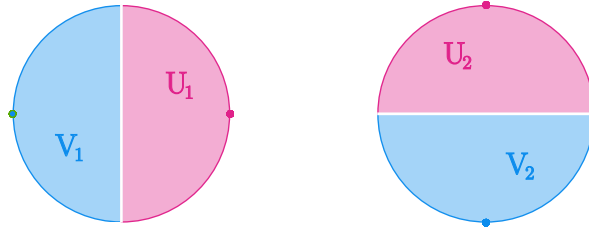


Fig. 2: : The projection of the northern hemisphere on the Poincaré disk, with charts U_1 , V_1 , U_2 and V_2 .

2.2 Application of the Poincaré compactification to predator-prey systems

In this subsection we obtain the Poincaré compactifications of systems (1) and (2).

2.2.1 A Kolmogorov system obtained from the Rosenzweig-MacArthur system

First, we consider (1) and we are going to obtain the expression of the compactification in the charts U_1 and U_2 . In this case, as the system is proposed in the field on population dynamics, and the variables only have biological meaning if they are non-negative, we are going to restrict the study of the orbits to the positive quadrant of the Poincaré disk. In any case it is necessary to study the compactification in the charts U_1 and U_2 , as the origin of U_2 is not included in the chart U_1 . Following the structure in system (3), for system (1) we have

$$P(x_1, x_2) = x_1(-x_1^2 + (1 - b)x_1 - x_2 + b) \quad \text{and} \quad Q(x_1, x_2) = x_2((c - \delta)x_1 - \delta b).$$

The degree of the equations is $d = 3$. According with the expression in (4), the compactification in chart U_1 is

$$\begin{aligned} \dot{u} &= uv^2 - b(\delta + 1)uv^2 + (b + c - \delta - 1)uv + u, \\ \dot{v} &= uv^2 - bv^3 + (b - 1)v^2 + v. \end{aligned} \tag{7}$$

This new expression of system (1) allows one to study the singular points at the infinity, which are those over the line $v = 0$. In this case the only infinite singular point in this chart is the origin of U_1 . The linear part of system (7) at the origin is the identity matrix, so O_1 is an unstable node as there are two positive eigenvalues.

We deal now with the compactification in chart U_2 . According with the expression in (5), system (1) in chart U_2 writes

$$\begin{aligned}\dot{u} &= -u^3 + (\delta + 1 - b - c)u^2v + b(\delta + 1)uv^2 - uv, \\ \dot{v} &= (\delta - c)uv^2 + b\delta v^3.\end{aligned}\tag{8}$$

We recall that we are interested in the phase portrait in the positive quadrant of the Poincaré disk. The only infinite point in the disk which is not covered by the chart U_1 is the origin of chart U_2 . Then we only need to determine if the origin of system (8) is a singular point. In this case, the origin is indeed a singular point, but in contrast to the origin of U_1 , the linear part of system (8) at O_2 is identically zero, so we need a desingularization technique to study it. In the following section we will introduce the blow up technique, and then we will deal again with this system.

Now we consider system (2). Again we will obtain the compactification in the local charts U_1 and U_2 , taking into account that for studying all the infinite singular points, it is enough to study the singular points over $v = 0$ in the chart U_1 and the origin of the chart U_2 . In this case we consider the complete Poincaré disk because, although in the case of the population dynamics the variables only have biological meaning when they are positive, these equations can be used in many other contexts, as explained in the Introduction, and in some of them it may make sense to consider negative values of the variables.

2.2.2 A Kolmogorov system obtained from the spatial Lotka-Volterra systems

System (2) is a polynomial system of degree 3 of the form (3) with

$$P(x_1, x_2) = x_1(a_0 + c_1x_1 + c_2x_2^2 + c_3x_2) \quad \text{and} \quad Q(x_1, x_2) = x_2(c_0 + c_1x + c_2x_2^2 + c_3z).$$

We start in this case with the study of the chart U_2 , which is simpler. According to equations (5) the system (2) in this chart has the expression:

$$\begin{aligned}\dot{u} &= (a_0 - c_0)uv^2, \\ \dot{v} &= -c_1uv^2 - c_0v^3 - c_3v^2 - c_2v.\end{aligned}\tag{9}$$

As we are interested in the infinite singular points, we study the singular points appearing over the line $v = 0$. In this case over this line we get that

$$\dot{u} |_{v=0} = \dot{v} |_{v=0} = 0,$$

and then all points at infinity are singular points, including the origin which is the only one we must study in this chart.

We see that the eigenvalues of the Jacobian matrix at the origin are zero and $-c_2$, therefore, it can be concluded that if $c_2 > 0$ there is exactly one orbit that goes from outside the infinity to the origin of the chart U_2 and if $c_2 < 0$ there is exactly one orbit that leaves the origin of U_2 and goes outside the infinity. This result is obtained with the results about normally hyperbolic surfaces. As it is not our objective here, we will not give more details, but interested readers can see [9].

Now we address the study of the infinite singular points in the local chart U_1 , where according to equations (4) the expression of the systems is

$$\begin{aligned}\dot{u} &= (c_0 - a_0)uv^2, \\ \dot{v} &= -c_2u^2v - c_3uv^2 - a_0v^3 - c_1v^2.\end{aligned}\tag{10}$$

Taking $v = 0$ we get again that all points at infinity in this chart are singular points. At any point $(u_0, 0)$ with $u_0 \neq 0$ the eigenvalues are one zero and the other $-c_2u_0^2$ so, with the same results mentioned for the origin of U_2 we can conclude that if $c_2 > 0$ exactly one orbit outside the infinity arrives at each infinite singular point on the chart U_1 distinct from the origin; and if $c_2 < 0$ from each infinite singular point on the chart U_1 distinct from the origin leaves exactly one orbit from outside the infinity.

However at the origin of chart U_1 the eigenvalues of the Jacobian matrix are both zero, so it is a linearly zero singular point. Again we will return to this problem after Section 3, in which we will introduce the blow up's.

3 A desingularization technique

The study of the dynamics around the singular points of a differential system is important as it can determine behaviors of practical interest, such as stabilization of populations at a certain level, or the extinction of some of the populations. However given the difficulty involved in the study of some of these points, we find in the literature that the study of the singular points is often omitted when they are not elementary.

In addition to the well known case of hyperbolic singularities, for the case of planar polynomial systems, there are very good results that give a complete classification in the semi-hyperbolic and nilpotent cases, i.e. when the eigenvalues of the Jacobian matrix at the singular points have one eigenvalue equal to zero or both equal to zero but the Jacobian matrix is not identically zero. These results can be found in Chapters 2 and 3 of [25].

The result for the nilpotent case in [25] is obtained by using the so called *homogeneous blow up's*. This technique is based essentially in the use of polar coordinates to transform the singular points which are nilpotent. As the result is completed in that case, and it can be directly applied to classify the nilpotent singular point determining the local behavior of the orbits, we will not give details about the proof, which can be found in [25].

However for the linearly zero singular points there are no results that allow us to classify them. Then we will give a short description on a technique that we have used in the context of population dynamics for the desingularization of these points: the *directional blow up's*.

3.1 Theoretical introduction of the directional blow up's

The basic idea behind this method is to convert the singular point that we want to study into a line. For doing that we do a change in the variables that “explodes” the singularity. The new singular points that appear on the line in which we have converted the singular point can be easier to study. If this is not the case, the process is repeated until we get to a system which does not have linearly zero singular points. Then we can study these singularities which are simpler and go back to our original system undoing the variable changes. This method is always valid since Dumortier demonstrated the finiteness of this iterative desingularization procedure (see [26]).

We introduce the directional blow up's for polynomial equations. To this end, we consider a differential system of the form

$$\begin{aligned}\dot{x} &= P(x, y) = P_m(x, y) + P_h(x, y), \\ \dot{y} &= Q(x, y) = Q_m(x, y) + G_h(x, y),\end{aligned}\tag{11}$$

where P and Q are coprime polynomials, P_m and Q_m are homogeneous polynomials of degree $m \in \mathbb{N}$ and P_h and Q_h are higher order terms in x and y . Our objective is to study the origin of this system, as it is a singular point since $m > 0$.

For a system of this form we call the polynomial

$$\mathcal{F}(x, y) := xQ_m(x, y) - yP_m(x, y),$$

the *characteristic polynomial* of system (11). With the directional blow up's we transform the origin of this system into a line, and we call that line the *exceptional divisor*.

3.1.1 Homogeneous vertical blow up

The *homogeneous directional blow up in the vertical direction* is the correspondence

$$(x, y) \rightarrow (x, z) = (x, y/x),$$

where z is a new variable. Then the exceptional divisor in this case is the line $x = 0$, as we transform the origin of system (11) into this line. After doing the variable change, the expression of the original system (11) is

$$\begin{aligned}\dot{x} &= P(x, xz), \\ \dot{z} &= \frac{Q(x, xz) - zP(x, xz)}{x},\end{aligned}\tag{12}$$

that is always well-defined since we are assuming that the origin is a singular point. In the obtained system, all the points at the exceptional divisor are singular points. The next step in this process is to cancel some common factors, more precisely:

- We cancel a common factor x^{m-1} if $\mathcal{F} \neq 0$.
- We cancel a common factor x^m if $\mathcal{F} \equiv 0$.

We have to take into account, while studying the transformation of the orbits, that in this kind of blow up, the variable change swaps the second and third quadrants with respect to the original system.

3.1.2 Homogeneous horizontal blow up

The *homogeneous directional blow up in the horizontal direction* is the correspondence

$$(x, y) \rightarrow (z, y) = (x/y, y),$$

where z is a new variable. The exceptional divisor in this case is the line $y = 0$, as we transform the origin of system (11) into this line. After doing the variable change, the expression of the original system (11) becomes

$$\begin{aligned} \dot{z} &= \frac{P(yz, y) - zQ(yz, y)}{y}, \\ \dot{x} &= P(yz, y), \end{aligned}$$

that is always well-defined since we are assuming that the origin is a singular point. As in the case of the vertical blow up, in the obtained system, all the points at the exceptional divisor are singular points, so we have to cancel some common factors, more precisely:

- We cancel a common factor x^{m-1} if $\mathcal{F} \neq 0$.
- We cancel a common factor x^m if $\mathcal{F} \equiv 0$.

Now, the quadrants that are swapped are the third and fourth quadrants, so we have to take this into account to studying the configuration around the original singular point.

Depending on the expression of the characteristic polynomial, the origin can be either a *nondicritical* singular point if $\mathcal{F} \neq 0$, or a *dicritical* singular point if $\mathcal{F} \equiv 0$.

In the dicritical case we have

$$P_m = xW_{m-1} \quad \text{and} \quad Q_m = yW_{m-1},$$

with $W_{m-1} \neq 0$ a homogeneous polynomial of degree $m-1$. If this polynomial W_{m-1} has a factor of the form $y - vx$ where $v = \tan \theta^*$, $\theta^* \in [0, 2\pi)$, then we say that θ^* is a *singular direction*.

The advantage of this method is that it allows one to study and determine the behavior of the solutions around the origin of our initial system (11), by studying the singular points of system (12) on the exceptional divisor, which can be of a simpler nature. If this does not occur, then some of the singular points on the exceptional divisor are linearly zero, and we can repeat the process until all the points obtained

are non-elementary. This method always works because it has been proven in [26] that this chain of blow ups necessary to get only elementary singular points is finite. We recall that singular points on the exceptional divisor we have to study, correspond to either characteristic directions in the nondicritical case, or singular directions in the dicritical case.

Once we have studied the dynamics around the exceptional divisor, to obtain the dynamics around the origin of the original system, we must undo the variable changes, taking into account the changes in the orbits and their orientations.

For example, if we have performed a blow up in the vertical direction, by undoing it, the third and fourth quadrants will swap their position and all the orbits arriving or leaving from a point that is on the exceptional divisor with the second coordinate equal to p , will become orbits arriving or leaving from the origin, respectively, with a slope p .

We must also study the flow over the axes in the original system, and combining the information, determine the sectors that appear in the phase portrait. The blow up's always determine the behavior of the orbits except, at most, around the exceptional divisor. For this reason, if when undoing the blow up we find some indeterminacy, it will be necessary to carry out a directional blow up in another direction. For example, if we have performed a blow up in the vertical direction, and we find an indeterminacy around the vertical axis of the original system, to solve it, it can be enough to perform a blow up in the horizontal direction.

The theoretical results that provide the relationship between the original singular point of system (11) and the new singularities of system (12) are the following: (for more details see [27]).

Proposition 2 *Let $\varphi_t = (x(t), y(t))$ be a solution of system (11) which tends to the origin when t goes to $\pm\infty$. Suppose that the origin of the system is a nondicritical singular point. Assume that φ_t is tangent to one of the two angle directions $\tan \theta = v$, $v \neq \infty$. Then the following statements hold.*

1. *The two angle directions $\theta = \arctan v$ (in $[0, 2\pi)$) are characteristic directions.*
2. *The point $(0, v)$ on the (x, z) -plane is an isolated singular point of system (12).*
3. *The solution φ_t corresponds to a solution of system (12) tending to the singular point $(0, v)$.*
4. *Conversely, any solution of system (12) tending to the singular point $(0, v)$ on the (x, z) -plane corresponds to a solution of system (11) tending to the origin in one of the two angle directions $\tan \theta = v$.*

Proposition 3 *Consider system (11) and suppose that the origin is a dicritical singular point. Then for every nonsingular direction θ there exists exactly one semipath tending to the origin in the direction θ in forward or backward time. If θ^* is a singular direction, there may be either no semipaths tending to the origin in the direction θ^* , or a finite number, or infinitely many.*

3.2 Application of the directional blow up's to predator-prey systems

3.2.1 A Kolmogorov system obtained from the Rosenzweig-MacArthur system

For system (1) we have studied the finite singular points in the positive quadrant, but this study is quite simple as the points turn out to be elementary. For this system, the origin $P_0 = (0,0)$ and the point $P_1 = (1,0)$ are singular points for any values of the parameters, and for some values a third singular point arises: $P_2 = (b\delta/(c-\delta), (-bc(\delta+b\delta-c))/(c-\delta)^2)$. In summary, we obtain the classification described in Table 1 for the finite singular points according to the values of the parameters b , c and δ . More details can be found in [11].

Case	Conditions	Finite singular points
1	$b\delta > c - \delta$.	P_0 saddle, P_1 stable node.
2	$b\delta = c - \delta$.	P_0 saddle, P_1 saddle-node.
3	$0 < b\delta < c - \delta$, $B \geq 0$, $A > 0$.	P_0 saddle, P_1 saddle, P_2 unstable node.
4	$0 < b\delta < c - \delta$, $B \geq 0$, $A < 0$.	P_0 saddle, P_1 saddle, P_2 stable node.
5	$0 < b\delta < c - \delta$, $B < 0$, $A > 0$.	P_0 saddle, P_1 saddle, P_2 unstable focus.
6	$0 < b\delta < c - \delta$, $B < 0$, $A < 0$.	P_0 saddle, P_1 saddle, P_2 stable focus.
7	$0 < b\delta < c - \delta$, $B < 0$, $A = 0$.	P_0 saddle, P_1 saddle, P_2 weak stable focus.

Table 1: The finite singular points in the closed positive quadrant for system (1).

However, for the study of infinite singular points, as we mentioned in Section 2, it is necessary to use some desingularization technique. More precisely, we need to desingularize the origin of the system in chart U_2 , i.e. the origin of

$$\begin{aligned}\dot{u} &= -u^3 + (\delta + 1 - b - c)u^2v + b(\delta + 1)uv^2 - uv, \\ \dot{v} &= (\delta - c)uw^2 + b\delta v^3.\end{aligned}\tag{13}$$

For doing that we use the blow-up technique. More precisely, we do a horizontal blow up introducing the new variable w_1 by means of the variable change $vw_1 = u$, and get the system

$$\begin{aligned}\dot{w}_1 &= v^2w_1^3 + (1 - b)v^2w_1^2 + bw_1v^2 - w_1v, \\ \dot{v} &= (\delta - c)w_1v^3 + b\delta v^3.\end{aligned}\tag{14}$$

Now rescaling the time variable we cancel the common factor v , getting the system

$$\begin{aligned}\dot{w}_1 &= vw_1^3 + (1 - b)vw_1^2 + bw_1v - w_1, \\ \dot{v} &= (\delta - c)w_1v^2 + b\delta v^2.\end{aligned}\tag{15}$$

Now the only singular point on $v = 0$ is the origin, which is semi-hyperbolic, so it is not necessary to do more chained blow up's. We can apply [25, Theorem 2.19]

and thus we conclude that it is a saddle-node. Studying the sense of the flow over the axis we determine that the phase portrait around the origin of system (15) is the one on Figure 3(a).

Now we start to undo the change. If we multiply by v , all the points of the w_1 -axis become singular points and the sense of all the orbits on the third and fourth quadrants is reversed. With these modifications we obtain the phase portrait for system (14), given in Figure 3(b).

After that we undo the blow up going back to the (u, v) -plane. We have to swap the fourth and third quadrants and compress the exceptional divisor into the origin. The phase portrait obtained for system (8) is not totally determined in the shaded regions of the third and fourth quadrants, see Figure 3(c).

As it was explained in the previous subsection, it can be solved by doing a vertical blow up but, in the case of this system, it is not necessary because we only need to know the phase portrait of O_2 in the positive quadrant of the Poincaré disc, which corresponds with the positive quadrant in the plane (u, v) , in which the phase portrait has been totally determined.

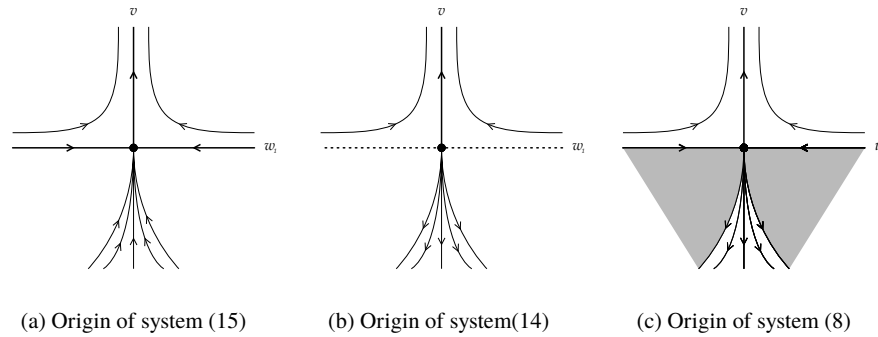


Fig. 3: Desingularization of the origin of system (8).

Finally, we have concluded that the local phase portrait at the origin of chart U_2 (which is an infinite singular point) is the same for all the values of the parameters: particularly, the origin of the chart U_2 has only one hyperbolic sector on the positive quadrant of the Poincaré disc being one separatrix at infinity and the other on $x = 0$.

The application of this technique is essential in order to complete the global classification of all the phase portraits of the system, which is included in Figure 4. More results and details about this system can be found in [11].

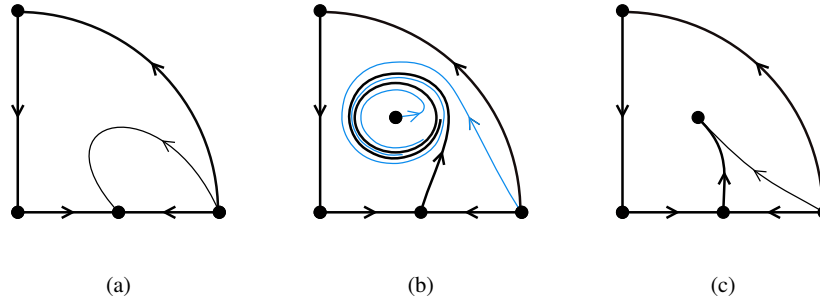


Fig. 4: Phase portraits of system (1) in the positive quadrant of the Poincaré disc.

3.2.2 A Kolmogorov system obtained from the spatial Lotka-Volterra systems

Let us now deal with system (2). For this system, as stated in Section 2, the singular point at the origin of the chart U_1 , which we will name O_1 , is linearly zero. For this singular point we will prove the following result.

Lemma 1 *The origin of the chart U_1 is an infinite singular point of system (2) and it has 12 distinct local phase portraits described in Figure 5.*

To prove Lemma 1 we use, among other results, the blow up technique. We illustrate now how is the proof of the result and how we can conclude by using directional blow up's. It is important to set that we work under the conditions

$$H = \{c_2 \neq 0, a_0 \geq 0, c_1 \geq 0, c_3 \geq 0, a_0 \neq c_0, a_0^2 + c_1^2 \neq 0\},$$

and the proof that this does not suppose any restriction in order to study all the dynamics, can be found in [9].

We recall that the system in chart U_1 has the expression

$$\begin{aligned} \dot{u} &= (c_0 - a_0)uv^2, \\ \dot{v} &= -c_2u^2v - c_3uv^2 - a_0v^3 - c_1v^2, \end{aligned} \tag{16}$$

and from these equations we can remove a common factor v obtaining:

$$\begin{aligned} \dot{u} &= (c_0 - a_0)uv, \\ \dot{v} &= -c_2u^2 - c_3uv - a_0v^2 - c_1v. \end{aligned} \tag{17}$$

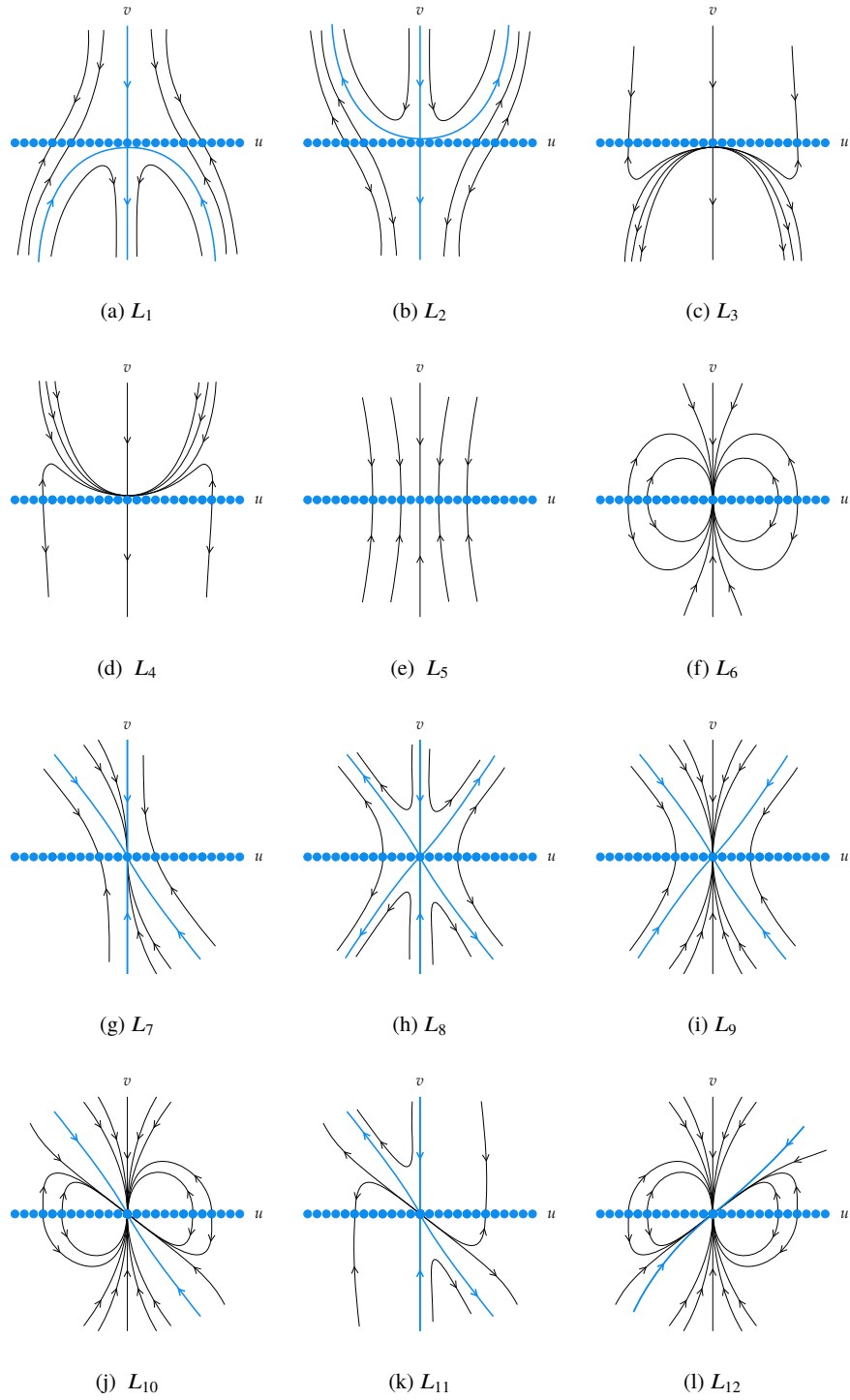


Fig. 5: Local phase portraits at the infinite singular point O_1 .

Then we study the only singular point over the exceptional divisor, i.e. over the line $v = 0$, the origin. We name this singular point \tilde{O}_1 . Now the eigenvalues of the Jacobian matrix at \tilde{O}_1 are zero and $-c_1$, so if $c_1 \neq 0$ the singular point of system (17) is semi-hyperbolic and we can study it applying Theorem 2.19 of [25]. The phase portraits corresponding with the semi-hyperbolic case are L_1 to L_4 in Figure 5, and more details can be found in [9].

Here we focus our attention in the case with $c_1 = 0$ in which we must do a desingularization process so we use the blow up technique.

We have to study which is the characteristic polynomial \mathcal{F} for system (17), and we obtain

$$\mathcal{F} = -c_2u^3 - c_3u^2v - c_0uv^2,$$

which can not be identically zero because $c_2 \neq 0$, so the singular point \tilde{O}_1 is nondicritical.

We introduce now a new variable w_1 trying to explode the singular point \tilde{O}_1 into a straight line, in particular, the line $u = 0$. We consider the variable change $uw_1 = v$, and making calculations we obtain the system

$$\begin{aligned} \dot{u} &= (c_0 - a_0)u^2w_1, \\ \dot{w}_1 &= -c_0uw_1^2 - c_3uw_1 - c_2u. \end{aligned} \tag{18}$$

With this variable change we have introduced a line filled up with singular points in the line $u = 0$ so, to remove it we must eliminate a common factor u , obtaining:

$$\begin{aligned} \dot{u} &= (c_0 - a_0)uw_1, \\ \dot{w}_1 &= -c_0w_1^2 - c_3w_1 - c_2. \end{aligned} \tag{19}$$

Now we focus our attention in the line $u = 0$, which is the exceptional divisor. The singularities over this line are the points with the first coordinate zero and the second one a solution of the equation $-c_0w_1^2 - c_3w_1 - c_2 = 0$. We must study all the singular points but, as they depend on the parameters, we should distinguish the following cases from (A) to (G).

- (A) If $c_0 = 0$ and $c_3 = 0$, as we are working under hypothesis H previously stated, and then $c_2 \neq 0$, there are no singularities with $u = 0$. We consider two cases depending on the sign of the parameter c_2 :

Subcase (A.1). Let $c_2 > 0$. Then system (19) has the phase portrait given in Figure 6(a). To undo the changes, the first step is to multiply by u , then all the points over the w_1 -axis become singular points, and the orbits on the second and third quadrants reverse their orientation. We obtain the configuration in Figure 6(b). Now we blow down, shrinking the exceptional divisor into the origin, and interchanging the second and third quadrants. Thus we obtain the phase portrait in Figure 6(c). Finally, to obtain the phase portrait of the initial system, we multiply by v , obtaining the phase portrait L_5 given in Figure 5, which has a line filled up with singularities, the u -axis.

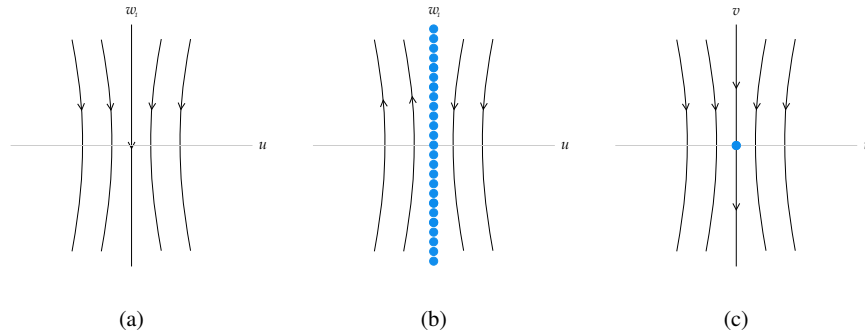


Fig. 6: Desingularization of the origin of systems (10) with $c_0 = c_1 = c_3 = 0$ and $c_2 > 0$.

Subcase (A.2). Let $c_2 < 0$. Then if we do a vertical blow up as in the previous case, it does not determine the configuration of the orbits. We only obtain the information that over the u -axis the flow is vertical and it goes in the positive sense. Therefore to obtain the complete phase portrait we do a horizontal blow up. We introduce a new variable w_2 with the change $vw_2 = u$, and with the hypothesis of this case we get the system

$$\begin{aligned} \dot{w}_2 &= c_2 w_2^3 v, \\ \dot{v} &= -c_2 w_2^2 v - a_0 v^2. \end{aligned} \quad (20)$$

If we remove a factor v in both equations we obtain

$$\begin{aligned} \dot{w}_2 &= c_2 w_2^3, \\ \dot{v} &= -c_2 w_2^2 - a_0 v. \end{aligned} \quad (21)$$

We study the singularities over the exceptional divisor, which in this case, as we have done a horizontal blow up, is the line $v = 0$. Over this line there is only one singular point, the origin, and it is a semi-hyperbolic singularity. We can use Theorem 2.19 in [25] to determine the phase portrait, and we obtain that it is a stable topological node. Then the phase portrait near the origin for system (21) is the one given in Figure 7(a).

If we multiply by the variable v , the phase portrait that we obtain for system (20) is the one in Figure 7(b).

To blow down we shrink the exceptional divisor into the origin and swap the third and fourth quadrants, so we get that in the first and second quadrants the orbits go to the origin tangent to the v -axis and in the third and fourth quadrants the orbits leave the origin tangent to the v -axis.

This qualitative behavior together with the information from the vertical blow up leads to the phase portrait in Figure 7(c).

Finally, we obtain the phase portrait for the initial system multiplying by v . The final result is the L_6 of Figure 5.

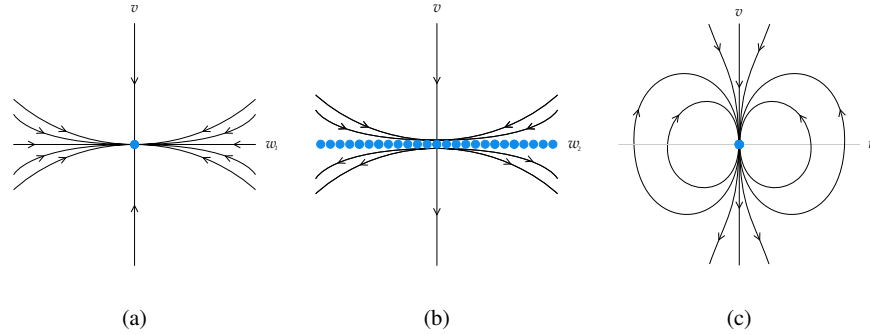


Fig. 7: Desingularization of the origin of systems (10) with $c_0 = c_1 = c_3 = 0$ and $c_2 < 0$.

(B) Let $c_0 = 0$ and $c_3 > 0$. Then over the exceptional divisor we have one singular point: $Q_1 = (0, -c_2/c_3)$. This singularity is hyperbolic and the eigenvalues of the Jacobian matrix are a_0c_2/c_3 and $-c_3$ so we have two subcases depending on their signs:

Subcase (B.1). If $c_2 > 0$ we do a horizontal blow up introducing the variable $vw_2 = u$ in systems (17), as with the vertical blow up we obtain some indeterminacies around the exceptional divisor. With the new variable w_2 we get

$$\begin{aligned} \dot{w}_2 &= c_2w_2^3v + c_3w_2^2v, \\ \dot{v} &= -c_2w_2^2v + c_3w_2v^2 - a_0v^2. \end{aligned} \tag{22}$$

Removing a common factor v , the system becomes:

$$\begin{aligned} \dot{w}_2 &= c_2w_2^3 - c_3w_2^2, \\ \dot{v} &= -c_2w_2^2v - c_3w_2v - a_0v. \end{aligned} \tag{23}$$

For this system we study the existence of singularities on the line $v = 0$, and we found two different points: the origin and the point $(-c_3/c_2, 0)$. The first one is a semi-hyperbolic saddle-node and the second one is a saddle.

Combining the phase portraits of both singularities the phase portrait for system (23) is the one in Figure 8(a).

If we multiply by v the phase portrait for system (22) is the one in Figure 8(b).

If we blow down we get the phase portrait in Figure 8(c) and finally, if we multiply again by v we obtain for the initial system the phase portrait L_7 of Figure 5.

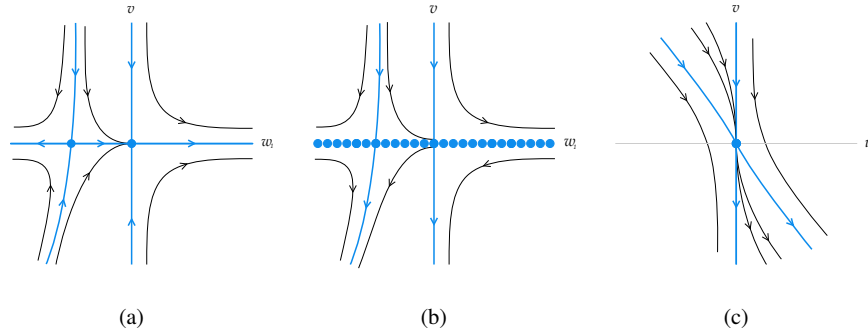


Fig. 8: Desingularization of the origin of systems (10) with $c_0 = c_1 = 0$, $c_3 > 0$ and $c_2 < 0$.

Subcase (B.2). In the case $c_2 < 0$ the singular point Q_1 is a stable node and we also need a horizontal blow up to determine the local phase portrait. The result obtained is the phase portrait L_6 of Figure 5.

- (C) Let $c_0 \neq 0$, $c_3 = 0$ and $c_0 c_2 > 0$. In this case there are no singularities over the exceptional divisor. We distinguish three subcases depending on the behavior of the orbits around that exceptional divisor. If c_0 and c_2 are positive we obtain the same phase portrait L_5 of Figure 5, and if c_0 and c_2 are negative, we obtain again the phase portrait L_6 of Figure 5, but in this case, to get to the final result, it is also necessary to do a horizontal blow up.
- (D) Let $c_0 \neq 0$, $c_3 = 0$ and $c_0 c_2 < 0$. Then over the exceptional divisor there are two hyperbolic singularities:

$$Q_2 = \left(0, \sqrt{\frac{-c_2}{c_0}}\right) \quad \text{and} \quad Q_3 = \left(0, -\sqrt{\frac{-c_2}{c_0}}\right).$$

Taking into account the eigenvalues of the Jacobian matrix at both points, we consider three subcases.

Subcase (D.1). If $c_0 > 0$ and $a_0 - c_0 > 0$, then the singular point Q_2 is a stable node and the singular point Q_3 is an unstable node. Undoing the blow up we obtain phase portrait L_6 of Figure 5.

Subcase (D.2). If $c_0 > 0$ and $a_0 - c_0 < 0$, then the singular points Q_2 and Q_3 are both saddle points with the orientation of the hyperbolic orbits given in Figure 9(a). If we multiply by u and then blow down, we obtain the phase portraits in Figure 9(b) and (c). Multiplying by u again we obtain that the local phase portrait for O_1 is L_8 of Figure 5.

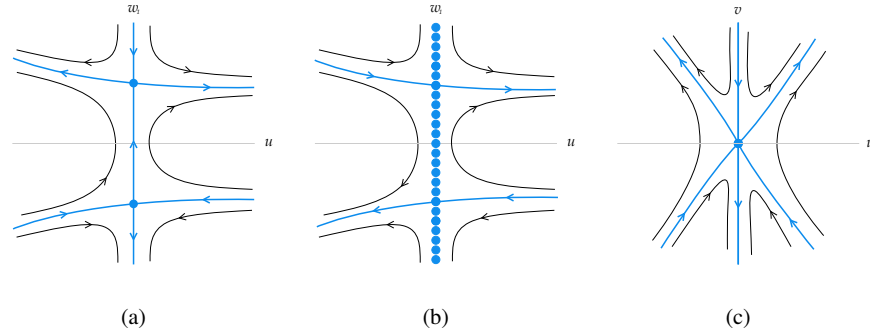


Fig. 9: Desingularization of the origin of systems (10) with $c_3 = 0$, $c_0 > 0$, $c_2 < 0$ and $a_0 - c_0 < 0$.

Subcase (D.3). If $c_0 < 0$ and $a_0 - c_0 > 0$, then the singular points Q_2 and Q_3 are both saddle points but with a different orientation than in case (D.2). Here the vertical blow up is not enough to determine the behavior of the orbits near the v -axis. We introduce the variable w_2 such that $vw_2 = u$, to explode the origin into a horizontal line. We obtain

$$\begin{aligned} \dot{w}_2 &= c_2 w_2^3 v + c_0 w_2 v, \\ \dot{v} &= -c_2 w_2^2 v - a_0 v^2, \end{aligned} \quad (24)$$

and then, removing a common factor v , we obtain

$$\begin{aligned} \dot{w}_2 &= c_2 w_2^3 + c_0 w_2, \\ \dot{v} &= -c_2 w_2^2 - a_0 v. \end{aligned} \quad (25)$$

For this system we study the singularities on the line $v = 0$, which are three: The origin which is a stable node, and two saddle points $(\pm\sqrt{-c_0/c_2}, 0)$. Combining these three singularities, the phase portrait around the w_2 -axis for system (25) is the one in Figure 10(a). If we multiply by v we get the phase portrait in Figure 10(b) for systems (24). Blowing down we obtain the phase portrait in Figure 10(c). If we multiply again by v we obtain the local phase portrait for O_1 which is L_9 of Figure 5.

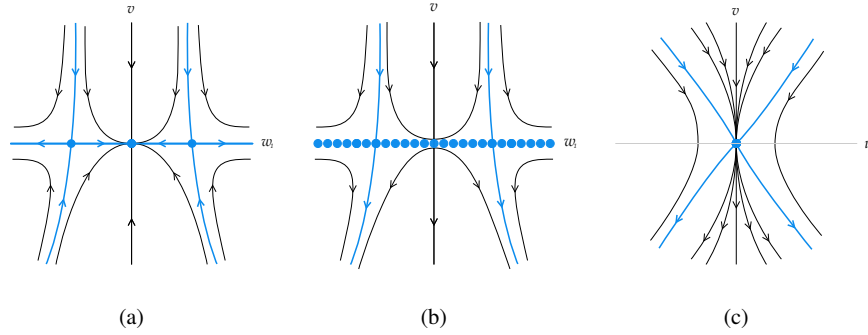


Fig. 10: Desingularization of the origin of systems (10) with $c_3 = 0$, $c_0 < 0$, $c_2 > 0$ and $a_0 - c_0 > 0$.

- (E) Let $c_0 \neq 0$, $c_3 \neq 0$ and $c_3^2 - 4c_0c_2 < 0$. In this case there are no singularities over $u = 0$. If $c_2 > 0$ the phase portrait is L_5 of Figure 5, and if $c_2 < 0$ we obtain, by combining with a horizontal blow up, the phase portrait L_6 of Figure 5.
- (F) Let $c_0 \neq 0$, $c_3 \neq 0$ and $c_3^2 - 4c_0c_2 > 0$. Then there are two hyperbolic singularities over $u = 0$:

$$Q_4 = \left(0, -\frac{c_3 + \sqrt{c_3^2 - 4c_0c_2}}{2c_0} \right) \quad \text{and} \quad Q_5 = \left(0, -\frac{c_3 - \sqrt{c_3^2 - 4c_0c_2}}{2c_0} \right).$$

Subcase (F.1). If $a_0 - c_0 > 0$, $c_0 > 0$ and $c_3^2 - 4c_0c_2 - c_3 > 0$, then Q_4 is an unstable node and Q_5 a stable node. Undoing the blow up we get the phase portrait L_6 of Figure 5.

Subcase (F.2). If $a_0 - c_0 > 0$, $c_0 > 0$ and $c_3^2 - 4c_0c_2 - c_3 < 0$, then the singular point Q_4 is an unstable node and the singular point Q_5 a saddle. Undoing the blow up we get the phase portrait L_7 of Figure 5.

Subcase (F.3). If $a_0 - c_0 > 0$, $c_0 < 0$ and $c_3^2 - 4c_0c_2 - c_3 > 0$, then the singular points Q_4 and Q_5 are saddle points, but the vertical blow up does not determine the behaviour of the orbits around the v -axis. Doing a horizontal blow up we obtain the phase portrait L_9 of Figure 5.

Subcase (F.4). If $a_0 - c_0 > 0$, $c_0 < 0$ and $R_c - c_3 < 0$, then Q_4 is a saddle and Q_5 is a stable node. Again the vertical blow up is not enough to determine the phase portrait. With a horizontal blow up we obtain the phase portrait L_{10} of Figure 5.

Subcase (F.5). If $a_0 - c_0 < 0$, $c_0 > 0$ and $R_c - c_3 > 0$, then Q_4 and Q_5 are saddle points. Undoing the blow up we get the phase portrait L_8 of Figure 5.

Subcase (F.6). If $a_0 - c_0 < 0$, $c_0 > 0$ and $R_c - c_3 < 0$, then Q_4 is a saddle and Q_5 is a stable node. Undoing the blow up we get the phase portrait L_{11} of Figure 5.

- (G) Let $c_0 \neq 0$, $c_3 \neq 0$ and $c_3^2 - 4c_0c_2 = 0$. In this case the singular point on the exceptional divisor is $Q_6 = (0, -c_3/(2c_0))$, and it is a semi-hyperbolic saddle-node. We have three different cases in which the position of the sectors of the saddle-node changes. These cases are determined by the signs of $c_0(a_0 - c_0) < 0$ and $c_0 < 0$. If $c_0(a_0 - c_0) > 0$ and $c_0 > 0$, we obtain the phase portrait L_7 , if $c_0(a_0 - c_0) < 0$ and $c_0 > 0$, we obtain the phase portrait L_{11} , and if $c_0(a_0 - c_0) < 0$ and $c_0 < 0$, we get the phase portrait L_{12} of Figure 5.

4 Conclusions

In this chapter we have presented, for two different predator-prey systems, some results about their global dynamics, paying special attention to the dynamics near the infinity and to the configuration of the orbits in a neighborhood of the nonelementary singular points.

First, in Section 2 we have used the Poincaré compactification, which is a very useful tool to study the behavior of the orbits which go or come from infinity. After a theoretical review of the technique, we have applied it to a Kolmogorov system obtained from a Rosenzweig-MacArthur system, and also to a Kolmogorov system obtained from a spatial Lotka-Volterra system. In the first case, we have obtained that there are only isolated singular points at the infinity, while in the second case, the infinity is formed by a continuum of singular points.

Then, in Section 3 we deal with the desingularization technique consisting on the use of the variable changes called blow up's. More precisely, we have used directional blow up's in the horizontal and vertical directions. This allows one to study any type of singularities of analytic systems in dimension two even if they are not elementary. We believe this is important since these type of singular points are not studied in many of the predator-prey systems proposed in the literature. In our case, we apply this technique to the study of singularities in the two planar Kolmogorov systems, giving a description of the process as well as a complete representation of all the results obtained.

Thus, the purpose of this chapter is twofold: on the one hand, to present the results we have obtained for these Kolmogorov systems, and on the other hand, to serve as an illustrative example of how the techniques used can allow a better study of some predator-prey systems proposed in the literature.

References

1. A. J. Lotka, *Elements of Physical Biology*, Waverly Press by the Williams and Wilkins Company, Baltimore, Md., U.S.A., 1925.
2. V. Volterra, *Variazione fluttuazioni del numero d'individui in specie animali conventi*, Atti della Accademia nazionale dei Lincei, **2** (1926), 31–113.

3. É. Diz-Pita and M. V. Otero-Espinar, *Predator-prey models: a review on some recent advances*, *Mathematics*, **9** (2021), 1783.
4. M. Rosenzweig and R. MacArthur, *Graphical representation and stability conditions of predator-prey interaction*, *The American Naturalist*, **97** (1963), 209–223
5. R. Huzak, *Predator-prey systems with small predator's death rate*, *Electronic Journal of Qualitative Theory of Differential Equations*, **86** (2018), 1–16.
6. A. Kolmogorov, *Sulla teoria di Volterra della lotta per l'esistenza*, *Giornale dell' Istituto Italiano degli Attuari*, **7** (1936), 74–80.
7. É. Diz-Pita, J. Llibre and M. V. Otero-Espinar, *Phase portraits of a family of Kolmogorv systems depending on six parameters*, *Electronic Journal of Differential Equations*, **35** (2021), 1–38.
8. É. Diz-Pita, J. Llibre and M. V. Otero-Espinar, *Planar Kolmogorov systems coming from spatial Lotka-Volterra systems*, *International Journal of Bifurcation and Chaos*, **31**(3) (2021), 2150201.
9. É. Diz-Pita, J. Llibre and M. V. Otero-Espinar, *Phase portraits of a family of Kolmogorv systems with infinitely many singular points at infinity*, *Communications in Nonlinear Science and Numerical Simulation*, **104** (2022), 106038.
10. É. Diz-Pita, J. Llibre and M. V. Otero-Espinar, *Planar Kolmogorov systems with infinitely many singular points at infinity*, *International Journal of Bifurcation and Chaos*, **32**(5) (2022).
11. É. Diz-Pita, J. Llibre and M. V. Otero-Espinar, *Global phase portraits of a predator-prey system*, *Electronic Journal of Qualitative Theory of Differential Equations*, **16**, 1–13.
12. F. H. Busse, *Transition to turbulence via the statistical limit cycle route*, *Synergetics*, **39** (1978), Springer-Verlag, Berlin.
13. R. Hering, *Oscillations in Lotka-Volterra systems of chemical reactions*, *J. Math. Chem.* **5** (1990), 197–202.
14. G. Gandolfo, *Economic dynamics*, Fourth edition. Springer, Heidelberg, 2009.
15. G. Gandolfo, *Giuseppe Palomba and the Lotka-Volterra equations*, *Rend. Lincei-Mat. Appl.*, **19**(4) (2008), 347–357.
16. A. W. Wijeratne, F. Yi and J. Wei, *Bifurcation analysis in the diffusive Lotka-Volterra system: an application to market economy*, *Chaos Solitons Fractals*, **40**(2), (2009), 902–911.
17. A. Arneodo, P. Couillet, P., C. Tresser, *Occurrence of strange attractors in three-dimensional Volterra equations*, *Phys. Lett.*, **79A**, 259–263.
18. J. Coste, J. Peyraud, P. Couillet, *Asymptotic Behaviors in the Dynamics of Competing Species*, *SIAM J. Appl. Math.* **36**(3), 516–543.
19. J. Llibre, D. M. Xiao, *Global dynamics of a Lotka-Volterra model with two predators competing for one prey*, *SIAM K. Appl. Math.* **74**(2), 434–453.
20. C. Lois-Prados, R. Precup, *Positive periodic solutions for Lotka-Volterra systems with a general attack rate*, *Nonlinear Anal.-Real World Appl.*, **52** (2020), 103024.
21. S. Smale, *On the differential equations of species in competition*, *J. Math. Biology*, **3** (1976), 5–7.
22. J. Alavez-Ramírez, G. Blé, V. Castellanos and J. Llibre, *On the global flow of a 3-dimensional Lotka-Volterra system*, *Nonlinear Anal.-Theory Methods Appl.*, **75** (2012), 4114–4125.
23. J. Llibre, Y. P. Martínez, *Dynamics of a family of Lotka-Volterra systems in \mathbb{R}^3* , *Nonlinear Analysis*, **199** (2020), 111915.
24. H. Poincaré, *Sur l'integration des équations différentielles du premier ordre et du premier degré I*, *Rendiconti del Circolo Matematico di Palermo*, **5** (1891), 161–191.
25. F. Dumortier, J. Llibre and J.C. Artés, *Qualitative Theory of Planar Differential Systems*, UniversiText, (Springer-Verlag, New York, 2006).
26. F. Dumortier, *Singularities of vector fields on the plane*, *Journal of Differential Equations*, **23** (1977), 53–106.
27. A. A. Andronov, E. A. Leontovich, I. J. Gordon and A. G. Maier, *Qualitative Theory of 2nd Order Dynamic Systems*, J. Wiley & Sons, 1973.